

# Characterization of the Reacting Flowfield in a Liquid-Fueled Stagnation Point Reverse Flow Combustor

P. Gopalakrishnan\*, M. K. Bobba\*, A. Radhakrishnan\*, Y. Neumeier<sup>∞</sup> and J. M. Seitzman\*

Guggenheim School of Aerospace Engineering  
Georgia Institute of Technology  
Atlanta, GA 30332-0150

**The Stagnation Point Reverse Flow (SPRF) combustor has been shown to operate stably while producing ultra-low NO<sub>x</sub> emissions over a range of loadings and equivalence ratios in both gas and liquid fueled operation. In nonpremixed gaseous operation, low NO<sub>x</sub> levels have been attributed to initial shielding of fuel from hot products allowing internal premixing of fuel and air to nearly the global equivalence ratio before burning. Various optical diagnostic techniques, such as chemiluminescence imaging and laser scattering, are employed to elucidate the combustion processes of this novel combustor in liquid-fueled operation. While the overall flow features are similar for both gas and liquid fuels, the combustion characteristics and NO<sub>x</sub> performance are strongly controlled by fuel dispersion and evaporation in liquid operation. Here, fuel dispersion is controlled by varying the placement of the fuel injector, which is centrally located within the annular air inlet tube. When the liquid injector is located in plane with the exit of the air annulus, the fuel remains initially shielded from the high temperature return products (similar to the gaseous case) producing a highly lifted flame. On the other hand, injecting the liquid upstream produces a more well-dispersed fuel pattern at the reactant inlet. This leads to a reduction of the equivalence ratio in the fuel consuming reaction zones. Hence the NO<sub>x</sub> emissions were found to be lower for this less shielded injector configuration over the range of global equivalence ratios and loadings investigated. Thus it is conjectured that the added delay caused by fuel evaporation before mixing and combustion can occur, changes the optimal shielding required for liquid-fueled operation.**

## I. Introduction

The drive towards reduced pollutant emissions has prompted the gas turbine industry to develop cleaner, more environmentally friendly power and propulsion systems, while simultaneously maintaining (or improving) efficiency, reliability and performance. The recently developed Stagnation Point Reverse Flow (SPRF) combustor has been demonstrated to produce low NO<sub>x</sub> emissions while operating with both gaseous and liquid fuels.<sup>[1-2]</sup> The combustor consists of a tube with one end open and the other closed. In the investigated configuration, the reactants are injected along the combustor center line, while the products flow in the reverse direction to exit the combustor, allowing the outflowing products and inflowing reactants to come into direct contact in a thin shear layer. The combustor has also been shown to operate stably over a wide range of flow rates and equivalence ratios. The geometry of the combustor ensures the existence of a low velocity stagnation region where the flame can stabilize. This coupled with the mixing of fuel and air with returning hot products and radicals allows this combustor to operate at very lean conditions over a range of loadings, without compromising stability.<sup>[3-6]</sup>

In gas-fueled operation, comparable NO<sub>x</sub> emissions were obtained for both premixed and nonpremixed modes. Comparison of the flowfields in the two modes of operation shows that velocity fields are similar except in a small region close to the injector exit. In premixed operation, a weakly attached flame was obtained, with some combustion in the jet shear layer but most of the reaction occurring far downstream. In the nonpremixed mode, the flame is highly lifted and stabilized in the third quarter of the combustor, which is characterized by low mean velocities and high turbulence levels. Similarity in NO<sub>x</sub> emissions for both operating modes has been attributed to

---

\* Graduate Research Assistant (AIAA Student Member)

<sup>∞</sup> Principal Research Engineer

\* Associate Professor (AIAA Associate Fellow)

efficient mixing of nearly all the fuel and air before burning. Since the fuel remains shielded from hot products by the coaxial air flow in nonpremixed operation, fuel and air internally premix to nearly the global equivalence ratio before combustion occurs.<sup>[7]</sup>

Although gaseous fuels are suitable in many instances, a number of applications require burning liquid fuels effectively while producing low emissions, e.g. aircraft turbine engines. Lean premixed, prevaporized combustion is a popular option to achieve low NOx emissions in liquid fueled systems. However, external prevaporization of liquid fuel is a serious safety hazard and adds extra complexity to the system. Relatively low NOx emissions have been achieved in the SPRF combustor with liquid fuels without external prevaporization through the use of a concentric injector design that relies on airblast atomization. This paper describes the effects of liquid-dispersion and fuel-product mixing on the performance and combustion characteristics of the SPRF combustor in liquid-fueled operation. To do so experimentally, non-intrusive optical diagnostic techniques such as chemiluminescence imaging, which acts as a marker of heat release rate,<sup>[8-12]</sup> and laser scattering from fuel droplets, which provides information on liquid fuel dispersion, are employed here. The integrated chemiluminescence signal is also analyzed to estimate the overall burning equivalence ratio in the combustor.<sup>[13-16]</sup>

## II. Experimental Set Up

The SPRF combustor used in the current study is a laboratory scale, atmospheric pressure device. It consists of a concentric injector centrally located in a 70 mm inner diameter quartz tube, which is closed at the bottom end with a quartz disk. The base plate is fit snugly inside the quartz tube so that there is no measurable leakage of fuel/air through the closed end. A tri-concentric injector design is employed for liquid-fueled operation. The fuel is pumped through a 500  $\mu\text{m}$  tube centered within a 6 mm tube with no flow in the outer region. The whole arrangement can be traversed inside a third concentric tube which forms an annular passage for air flow. The fuel tube is centered with respect to the outer air annulus using set-screws. The air stream surrounding the fuel facilitates atomization of the fuel jet. Care is also taken to ensure that the whole injector is centered with respect to the combustor. Air flow rate is monitored and controlled using a calibrated rotameter. The fuel flow rates are calculated based on measurements of excess oxygen in the product gases with a portable gas analyzer (Horiba CEMS - PG250). The gas analyzer also measures the NOx emissions from the combustor. The temperature of the exhaust gas is monitored simultaneously with an unshielded K-type thermocouple. As the inlet air is not preheated, the combustor is ignited with a premixed mixture of natural gas and air and the liquid fuel is introduced gradually before switching to fully liquid operation. In this study, two separate fuel tube locations have been investigated – (1) liquid fuel injector is flush with the exit of the air injector (denoted by 0") and (2) liquid fuel injector is retracted to 3.25" above the exit of the air injector (denoted by -3.25").

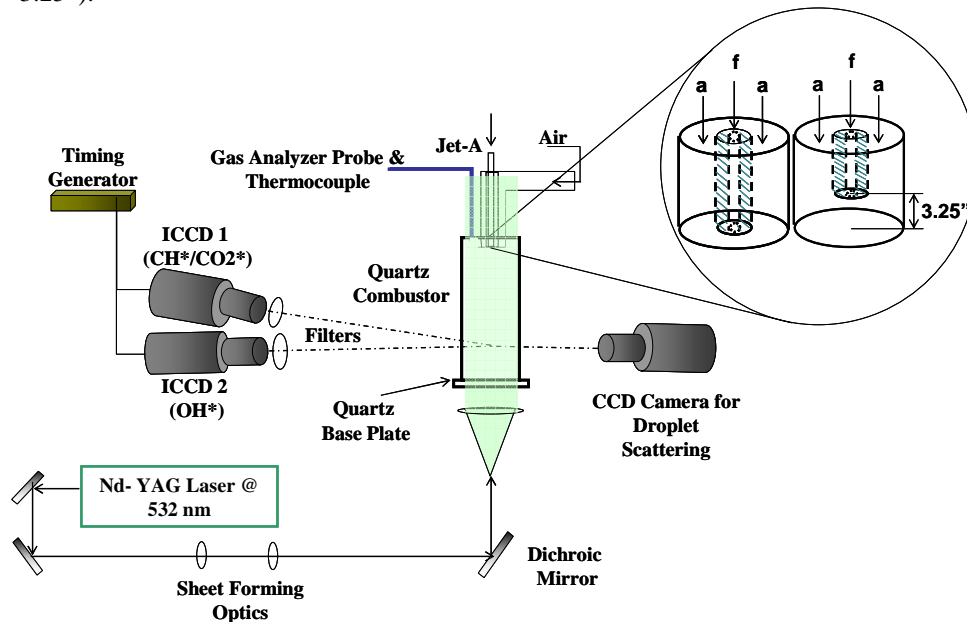


Figure 1. Experimental set-up for droplet scattering and  $\text{CH}^*/\text{CO}_2^*/\text{OH}^*$  chemiluminescence imaging.

### Simultaneous Droplet Scattering and CH\* Chemiluminescence

As shown in Figure 1, the location of liquid fuel in the combustor is visualized by illuminating the fuel jet with a laser light sheet produced from the 2<sup>nd</sup> harmonic output of a dual-head, pulsed Nd:YAG laser (Surelite I-10). The laser beam is converted into a thin sheet (~0.4 mm thick) 65 mm wide with two cylindrical lenses and enters the combustor from the closed end. The scattered light is detected normal to the laser sheet with a 12-bit interline CCD camera (MicroMAX, 1300×1030 pixels) and a 50 mm, f 1/1.8 camera lens.

Chemiluminescence emission has commonly been used as a measure of chemical reaction rates as well as heat release rates and provides information on the presence and strength of the combustion processes in a specific region of a combustor. Chemiluminescence intensities relate to rates of production and depletion of the particular species. These rates vary with reaction pathways which is a function of equivalence ratio. Hence, the equivalence ratio can be deduced from signal intensities.<sup>[13-16]</sup> In this study, an intensified camera (Princeton Instruments ICCD-576-S/RB-E, 18 mm intensifier, 384×576 pixels) and interference filter (430±5 nm) is used to collect CH\* chemiluminescence and a portion of the CO<sub>2</sub>\* chemiluminescence that occurs in the same spectral region. The intensifier gate of the second camera is synchronized with the droplet scattering system, such that the exposure begins 100 ns after the Nd:YAG laser pulse and lasts 250 μs. The chemiluminescence camera is also mounted at right angles to the laser sheet. Thus nearly simultaneous imaging of fuel droplets and chemiluminescence is achieved.

### Simultaneous OH\* and CH\* Chemiluminescence

Separately, OH\* chemiluminescence measurements are obtained with a second intensified camera (PI-MAX, 1024×256 pixels) equipped with a UV-Nikkor lens (105mm, f/4.5) with a Schott glass filter (WG308) placed in front of the lens. CH\*-CO<sub>2</sub>\* chemiluminescence is imaged with the same camera and filter set-up described previously. During this experiment, the droplet scattering system is disabled and the two intensified cameras are synchronized with a DG-535 pulse generator. The cameras are aligned such that the angle between them is as small as possible and their fields of view are matched to include the entire length and width of the combustor.

## III. Results and Discussion

As noted previously, one of the key features of the SPRF combustor is its ability to run stably over a range of equivalence ratios and loadings while producing ultra low NO<sub>x</sub> emissions with both gaseous and liquid fuels. Figure 2 shows a comparison of the NO<sub>x</sub> emissions obtained with (liquid) Jet-A and natural gas as fuels. As seen in the figure, the performance of the combustor in liquid-fueled operation is dependent on both the operating conditions as well as the location at which liquid fuel is injected. The emissions are found to be lower when the liquid injector is retracted into the air annulus (Legend: -3.25") compared to when it is level with the air exit (Legend: 0"). This trend is observed over the entire range of temperatures and flow rates investigated. Also, a reduction in NO<sub>x</sub> emissions is observed when the flow rates are increased. This effect is more pronounced at temperatures above 1800K. The NO<sub>x</sub> levels obtained in gaseous operation under similar operating conditions are also plotted in Figure 2 for comparison. Several similarities are found between the two modes of operation. In gas-fueled operation, it is observed that premixed and nonpremixed operation produce nearly the same NO<sub>x</sub> levels at low temperatures (below ~1900K). Beyond this, the nonpremixed mode produces higher emissions. The same is true when the liquid is injected level with the air annulus. In addition, we see a decrease in NO<sub>x</sub> emission with an increase in loading at high temperatures for gas fueled operation. This result is more pronounced in the nonpremixed mode as compared to the premixed mode. Likewise, in liquid operation, for temperatures below 2100 K, the effect of loading on NO<sub>x</sub> emissions is small when the liquid is injected well inside the air annulus. A possible explanation for these similarities is that when

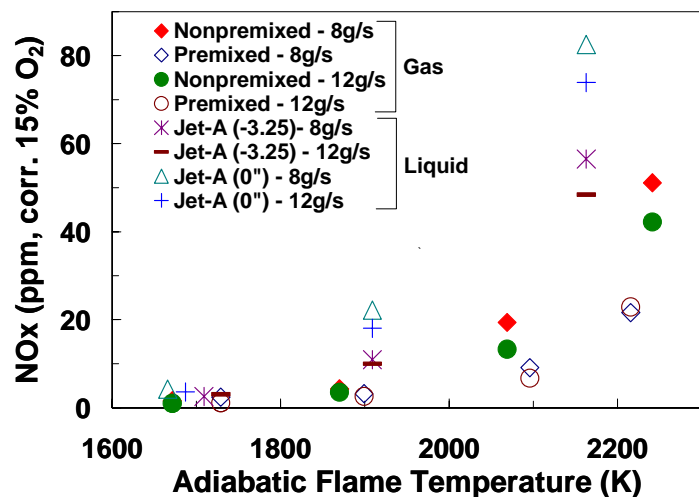


Figure 2. Variation of NO<sub>x</sub> emissions with adiabatic flame temperature.

the fuel is injected far upstream, the liquid jet can spread inside the injector and interact with the air causing some premixing of air and fuel to occur whereas when the liquid is injected at the exit of the air annulus, the two flows remain completely separated until they enter the combustor analogous to gaseous nonpremixed operation. To better understand the performance of the combustor in liquid-fueled operation, the remainder of this paper investigates the flowfield and combustion characteristics in this mode of operation through the use of various optical diagnostic techniques.

The effects of fuel injector placement on fuel dispersion are shown in Figure 3. In both injector configurations, droplet scattering images show the presence of a significant amount of liquid at the combustor inlet. Thus, the fuel is not vaporized in spite of hot product gases flowing over the injector. However, the dispersion of liquid changes significantly depending on the location at which the fuel is injected. When the liquid injector is level with the exit of the air annulus, the fuel enters the combustor as a liquid jet which gradually breaks up to form droplets. As seen in Figure 3(a), the liquid remains in the center mostly shielded from the hot products by the surrounding air until ~50mm below the injector exit. Further downstream, as the jet spreads, significant product entrainment occurs causing the fuel droplets to evaporate and burn. The variation in the average droplet intensities (radially integrated across the width of the jet) along the length of the combustor is plotted in Figure 3c. When the liquid injector is flush with the air exit, the average intensity is roughly constant initially before decreasing downstream. This behavior is attributed to the dependence of the scattered light intensity on the liquid morphology. Close to the injector exit, the liquid forms a jet that likely undergoes little evaporation. However, downstream, as the jet breaks up to form droplets, the scattered intensity begins to decrease and this continues as the droplets evaporate. On average it is seen that fuel droplets penetrate approximately 220 mm downstream of the injector.

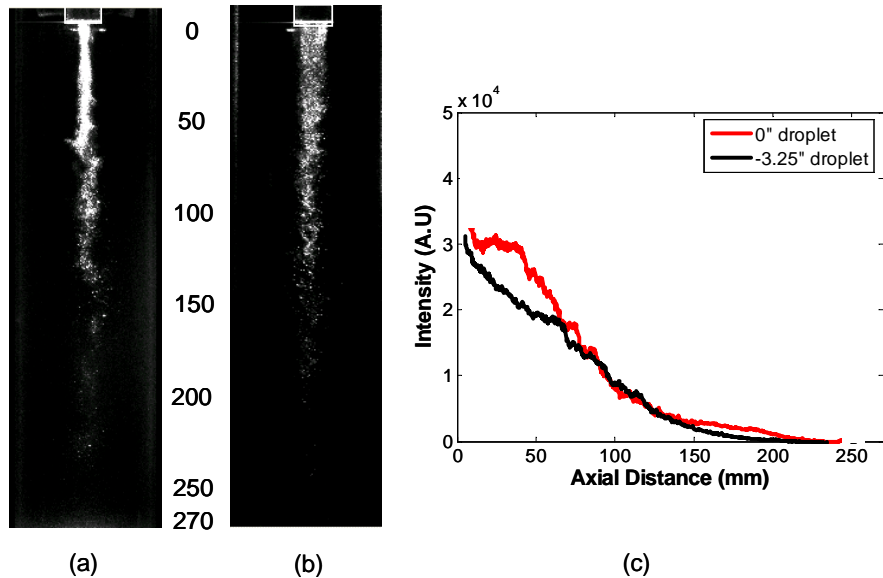


Figure 3. Instantaneous droplet scattering images at global  $\phi=0.5$  and  $m_{air} = 8g/s$ . (a) Liquid injector 0" (b) Liquid injector -3.25" (c) Variation of averaged (binned) intensities with distance from injector exit.

When the fuel injector is retracted into the air tube, the liquid fuel entering the combustor is no longer in the form of a jet. Rather, the fuel exits the injector as droplets that are spread out over the entire width of the injector. Since the atomization velocities are comparable in both cases, this difference in fuel distribution is mainly attributed to the spreading of the liquid jet across the injector. Hot product gases flowing over the air inlet tube also preheat the air, thus some of the fuel could be evaporated within the air tube. Also since some of the fuel is at the edge of the inlet air jet, all the fuel is no longer shielded by the air and even more fuel can evaporate as the incoming air and exiting hot products mix. This is likely the reason why the scattering signal drops more quickly in the upstream portion of the combustor for the retracted case compared to the flush case. In summary in the retracted case, the fuel is better dispersed and more quickly vaporized. Thus it can mix with air and products to produce a lean mixture before combustion occurs. However, when the liquid is injected at the exit, combustion is partially limited by the evaporation rate of the liquid fuel and is more likely to be characterized by higher equivalence ratios at the fuel consuming reaction zone.

Next, we examine the effect of fuel distribution on the flame characteristics. The mean  $\text{CH}^*$  (and  $\text{CO}_2^*$ ) chemiluminescence field for a global equivalence ratio ( $\phi$ ) of 0.5 and an air mass flow rate of 8 g/s is shown in Figure 4 for the two injector configurations. As seen from the figure, the location of the heat release zone varies significantly depending on the position of the fuel injector. When the fuel is injected at the exit of the air annulus, a highly lifted flame is observed (Figure 4a). No significant heat release is seen until approximately 100 mm downstream of the injector; a majority of the heat release occurs between 160–240 mm (recall, the full combustor length is 300 mm). The lack of heat release near the injector exit is consistent with the fuel distribution seen in Figure 3; with the fuel centrally located and shielded from the hot products, no combustion can occur until further downstream when sufficient mixing has occurred. On an instantaneous basis, the flame is highly unsteady with significant flapping in the radial direction. These observations are similar to the flame features obtained in nonpremixed gaseous operation of the combustor (Figure 4(c)).

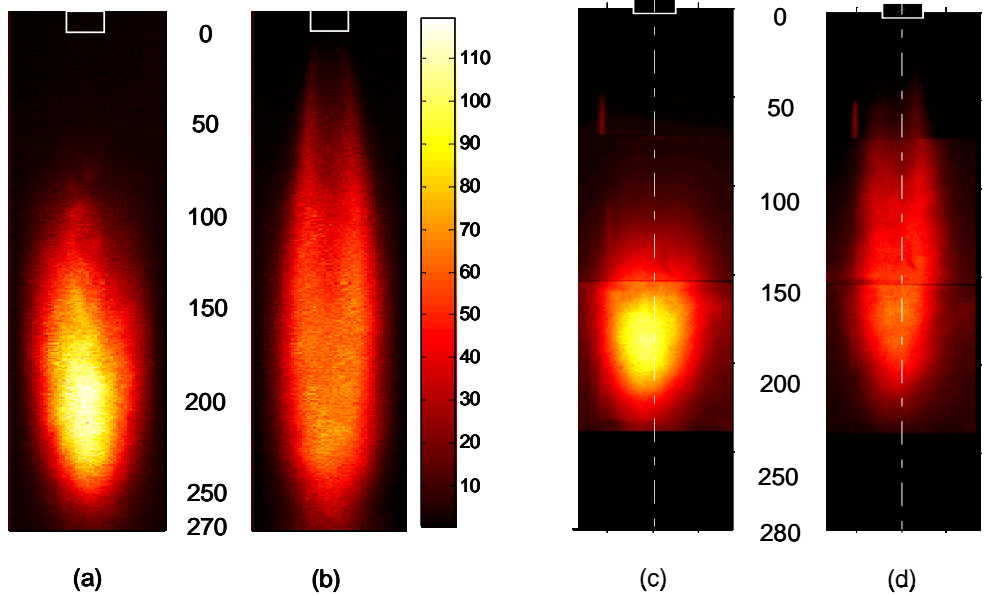


Figure 4. Conditionally averaged  $\text{CH}^*$  chemiluminescence signal for global  $\phi=0.5$  and  $m_{\text{air}} = 8\text{g/s}$ : (a) Liquid injector : 0" (b) Liquid injector : -3.25" (c) Gas fueled nonpremixed mode (d) Gas fueled premixed mode.

When the injector is retracted however, heat release begins closer to the injector and extends to the same downstream region as the flush injector case. The near field heat release can occur because some of the fuel is now located along the edge of the inlet jet, where mixing with air and hot products leads to a flammable mixture. The low chemiluminescence intensities in this region indicate the presence of a highly strained attached flame in the near field shear layer between the incoming reactants and exiting products. A similar shear layer flame region is observed for premixed gas-fueled operation (at the same air mass flow rate). However, the flame extends closer to the injector in the liquid fueled case. This may be partly attributed to the lower strain produced when the liquid injector is moved upstream. This placement increases the exit flow area by  $\sim 33\%$ , which in turn lowers the exit velocity of the reactant mixture by a similar amount. Based on the instantaneous images, the flame exhibits less radial flapping in this configuration but has a greater intermittency close to the injector. Presumably the intermittency is associated with the strain and mixture variability in the shear layer between the reactants and returning products close to the injector exit. To account for this, the mean  $\text{CH}^*$  field is obtained by averaging the instantaneous data conditioned on a chemiluminescence signal above the background noise.

Based on the overall chemiluminescence/heat release images, the combustor operating with the retracted liquid fuel injector, with its greater initial fuel dispersion, more closely resembles operation with gaseous fuel when the

Injector Location	$\text{CH}^*$ signal (arb units)	$\text{OH}^*$ signal (arb units)
Flush: 0"	2.29	2.14
Retracted: -3.25"	2.20	1.74

Table 1. Integrated chemiluminescence signal for global  $\phi=0.5$  and  $m_{\text{air}} = 8\text{g/s}$

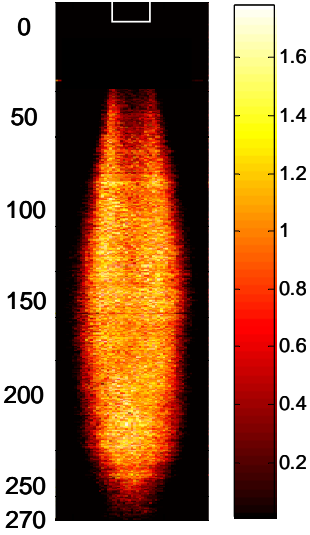


Figure 5. Average CH\*/OH\* ratio for  $\phi=0.5$ ,  $m_{\text{air}} = 8\text{g/s}$  and liquid injector:  $-3.25''$ .

reactants are premixed (as opposed to when they are nonpremixed). Thus it may be surmised that pulling the liquid injector back causes the combustor to behave more like a premixed system. To verify this, conditionally averaged CH\* and OH\* chemiluminescence signals were integrated over the volume of the combustor for the two injector configurations. The data (Table 1), reveals that the total CH\* and OH\* signal is lower for the retracted case, with a greater fractional change seen for the OH\* emission. It should be noted that the chemiluminescence data presented here has not been corrected to remove background due to CO<sub>2</sub>\* radiation.

It has previously been shown that integrated CH\* and OH\* chemiluminescence intensities for a given mass flow rate of fuel and air increase slightly with equivalence ratio for  $\phi < 0.7$  in n-heptane.<sup>[15-16]</sup> Since Jet-A and heptane are both similar higher order hydrocarbons, the chemiluminescence behavior is not expected to change drastically. However, the change in OH\* signal observed here is significantly higher than expected. This may be due to a high CO<sub>2</sub>\* background compared to the OH\* signal. Hence the lower signal intensity obtained when the liquid injector is retracted can be interpreted as leaner overall burning equivalence ratios compared to the flush case. This is also consistent with the observations from the droplet scattering data presented earlier. Therefore, when the liquid is injected well inside the air annulus and the fuel is dispersed across the inlet, vaporization and partial premixing of air and fuel occur more rapidly than when the fuel is confined within the center of the air jet. The enhanced mixing of vaporized fuel and air leads to leaner fuel-air mixtures in the primary reaction zones resulting in the lower measured NO<sub>x</sub> emissions. In gaseous nonpremixed operation of the SPRF combustor, low NO<sub>x</sub> levels have been attributed to initial shielding of fuel

from hot products, which allows the fuel and air to internally premix to nearly the global equivalence ratio before combustion occurs. However, in liquid operation, the additional time required to evaporate the fuel reduces the necessity to shield the fuel.

An estimate of the spatial distribution of equivalence ratio for this injector configuration is obtained by taking the ratio of the CH\* to OH\* chemiluminescence signals. For other fuels, it has been shown that the CH\*/OH\* ratio generally increases with equivalence ratio, at least for near stoichiometric and lean mixtures. As seen from Figure 5, the CH\*/OH\* ratios tend to remain almost constant over the entire heat release region with slightly higher ratios in the shear layer close to the injector exit. These results suggest that there is only a small variation in equivalence ratio across most of the combustor, with slightly richer combustion close to the injector, where there has been less time for fuel-air mixing.

As the fuel flow rate is increased while maintaining the same air flow rate, so that overall equivalence ratio is increased to 0.75, the flowfield of the combustor changes significantly. The averaged chemiluminescence data (Figure 6) show a more compact heat release zone compared to the global  $\phi = 0.5$  case for both the injector configurations. As the equivalence ratio increases, the resulting temperature increase causes the overall reactivity of the various species to go up. Consequently, a shorter and more stable flame is obtained at higher equivalence ratios. So instantaneously the flame does not exhibit significant radial flapping and remains confined to central portion of the combustor resulting in a narrowing of the overall heat release zone. When the injector is pulled up, the intermittency close to the injector exit is greatly reduced for the high  $\phi$  case (compared to low  $\phi$ ). A comparison of the integrated CH\* and OH\* chemiluminescence intensities for the two injector configurations shows a ~23% reduction in the signal when the fuel injector is retracted. However, the CH\* and OH\* data for heptane indicate that the integrated signal remains nearly constant between  $\phi = 0.75-1$ <sup>[15]</sup> (though this is based on background corrected CH\* and OH\* chemiluminescence signals). As the temperature increases, the background due to CO<sub>2</sub>\* radiation is

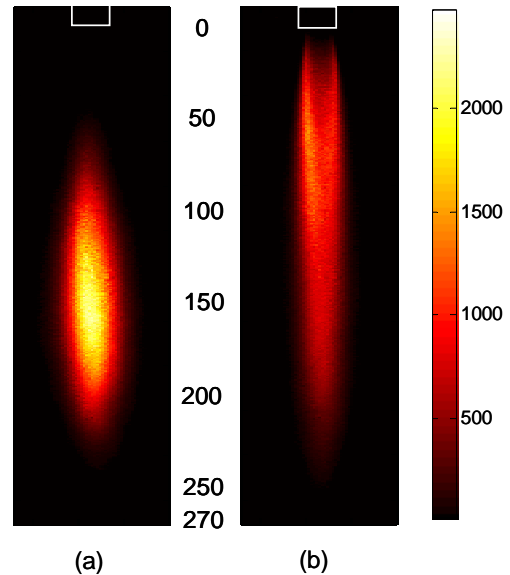


Figure 6. Average CH\* chemiluminescence signal for global  $\phi=0.75$  and  $m_{\text{air}} = 8\text{g/s}$ : (a) Liquid injector:  $0''$  (b) Liquid injector:  $-3.25''$ .

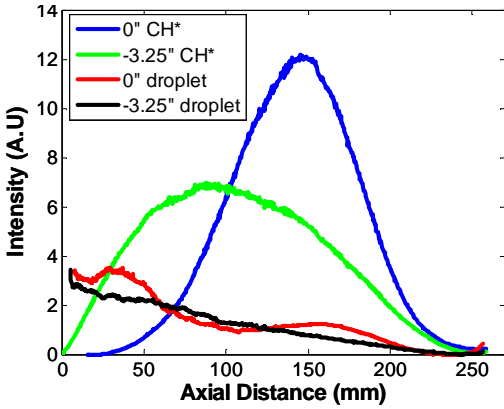


Figure 7. Variation in CH\* signal and scattered intensities with axial distance for  $\phi=0.75$ ,  $m_{air}=8\text{g/s}$ .

expected to increase. Hence the change in integrated signal observed here could be a result of this background. It is therefore not possible to conclude that the overall burning equivalence ratio is lower for the retracted case at high  $\phi$  based on the chemiluminescence data. Although, the lower NOx emissions obtained in this configuration suggest this.

Figure 7 shows the variation in radially integrated droplet intensities as well as the chemiluminescence signal with axial distance from the injector exit. When the fuel tube is flush with the air annulus, we see an increase in the integrated scattering intensities close to the injector before dropping off further downstream. This coincides to the region where the liquid jet breaks up to form droplets. There is a continuous drop in the intensities beyond  $\sim 40\text{mm}$ , at which point the heat release starts to pick up. When the fuel injector is retracted the liquid fuel is well atomized and enters the combustor mostly in the form of droplets. For this case, the immediate rise in heat release due to the presence of a

near field shear layer flame causes a steady decrease in droplet intensity through the length of the combustor.

Finally, we examine the effect of loading on the combustion characteristics and performance of the combustor at constant equivalence ratio. The location of the heat release zone at different loadings is shown in Figure 8 for the two injector configurations. At higher flow rates, the heat release region is more spread out for both injector locations. A comparison of the total chemiluminescence intensity at high loading shows that the integrated signal is higher when the liquid injector is retracted. This difference is probably due to the increased  $\text{CO}_2^*$  radiation at high loadings.

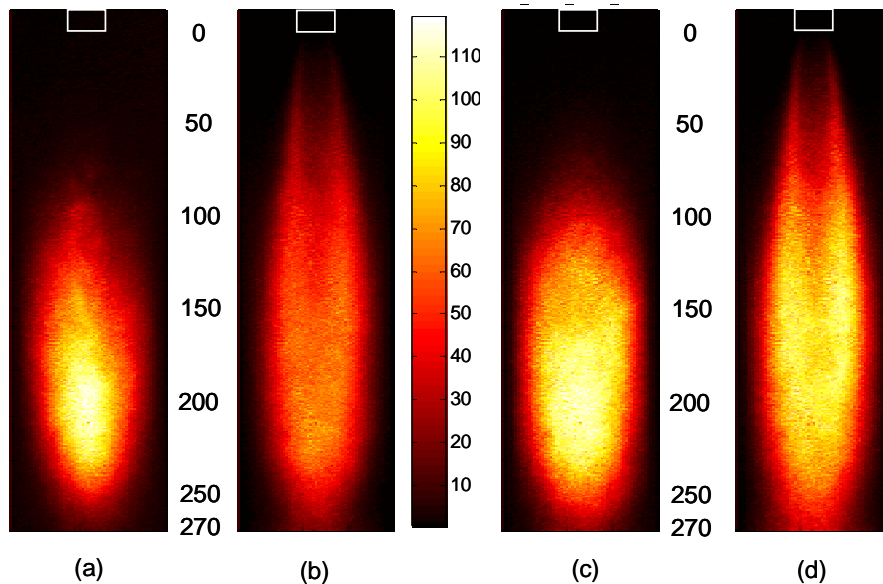


Figure 8. Average CH\* chemiluminescence signal for a global  $\phi=0.5$  and  $m_{air} = 8 \text{ g/s}$ : (a) Liquid injector: 0" (b) Liquid injector: -3.25" and  $\phi=0.5$ ,  $m_{air} = 12 \text{ g/s}$ : (c) Liquid injector: 0" (d) Liquid injector: -3.25"

The overall chemiluminescence signals are higher when the loading is increased. This is expected as both CH\* and OH\* chemiluminescence signals should increase roughly linearly with fuel flow rate, all other conditions being constant. In this case, when the loading was increased at a constant overall  $\phi=0.5$ , the mass flow rate of Jet-A increased by  $\sim 50\%$ . The variation in the total, spatially integrated signal is shown in Figure 9. With the injector retracted, the CH\* ( $+\text{CO}_2^*$ ) signal increases by nearly the expected  $\sim 50\%$ , but for the flush injector case, the CH\* emission only increases by  $\sim 32\%$ .

This may be interpreted as a general reduction in the fuel-air ratio in the heat release zone at high loading for the flush injector case. Less influence of loading is seen for the retracted injector. Thus the change in the burning equivalence ratio is not as pronounced when the injector is retracted. These observations are in agreement with the NO<sub>x</sub> data presented earlier where loading showed a greater effect on NO<sub>x</sub> emissions for the flush injection.

At higher overall equivalence ratios, a more significant effect of loading on NO<sub>x</sub> emissions was observed. In addition, both injector locations demonstrated similar behavior. At the higher overall fuel-air ratios, it is expected that thermal NO<sub>x</sub> becomes the dominant source. Thus increased loading (flow rate) also corresponds to a reduced residence time of the combustion products inside the combustor, which would reduce the NO<sub>x</sub> levels at the combustor exit.

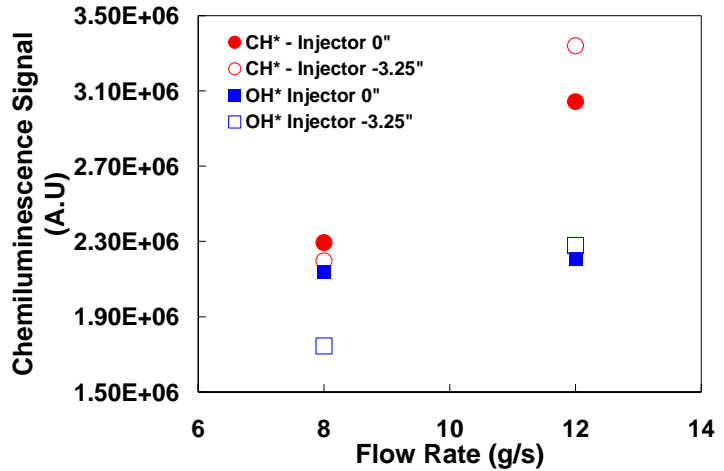


Figure 9. Variation in integrated chemiluminescence signal with loading for a global  $\phi=0.5$ .

#### IV. Conclusions

The combustion characteristics of the SPRF combustor in liquid-fueled operation were investigated for different fuel injector configurations. Non-intrusive optical diagnostic techniques, laser scattering and chemiluminescence imaging, were employed to analyze the fuel distribution and to characterize the combustion processes in the combustor. NO<sub>x</sub> emissions from the combustor were measured for various operating conditions and the observed trends can be explained based on the flowfield data. It is seen that although the overall flow features are similar in both gaseous and liquid-fueled operation, the NO<sub>x</sub> performance is mainly controlled by the fuel dispersion and evaporation rates in the latter.

The effect of fuel distribution on the flowfield of the combustor is investigated by varying the location at which the liquid fuel is injected, thus altering the spray pattern as well as the extent of fuel-product shielding in the combustor. When the liquid injector is flush with the air annulus, fuel enters the combustor in the form of a liquid jet surrounded by the annular air stream. Shear provided by the high velocity annular air flow facilitates atomization of the liquid jet and also shields it initially from the high temperature return flow. In this configuration, a highly lifted flame is observed where most of the heat release occurs in the third quarter of the combustor. When the fuel injector is retracted, the liquid fuel is well dispersed across the inlet air jet, and the heat release region moves closer to the injector. For this injector placement, the integrated chemiluminescence signals are found to be lower than in the flush case indicating that combustion occurs at a leaner overall equivalence ratio. Thus when the liquid fuel is dispersed across the inlet air, a lean mixture of fuel, air and hot products can be formed, resulting in the lower measured NO<sub>x</sub> emissions. For both fuel injector locations, increasing the global equivalence ratio by increasing the fuel flow rate results in increased reactivity of the mixture and produces a more compact heat release region that is located closer to the injector exit. The effect of loading on the combustion characteristics and NO<sub>x</sub> performance was also investigated for the different injector configurations. Comparison of the integrated chemiluminescence signal indicates a slightly lower burning equivalence ratio at high flow rates. This together with the lower residence times results in a reduction in NO<sub>x</sub> emissions at high loadings.

In summary, the SPRF combustor has been shown to operate stably with nonpre-vaporized Jet-A while producing low NO<sub>x</sub> emissions. While the low NO<sub>x</sub> levels in nonpremixed gaseous fuel operation is attributed to complete shielding of fuel from products initially, so as to allow internal premixing of fuel and air, in liquid-fueled operation, the additional time required for evaporation reduces the need for fuel-product shielding.

#### V. References

- <sup>1</sup> Y. Neumeier, B. Zinn, Y. Weksler, J. Seitzman, J. Jagoda, and J. Kenny (2005) "Novel Combustor for Ultra Low Emissions with Non-Premixed Reactants Injection," AIAA-2005-3775 Joint Propulsion Conference, July 2005 Tucson, Arizona.

<sup>2</sup> J. Crane, Y. Neumeier, J. Jagoda, J. Seitzman and B. Zinn, "Stagnation-Point Reverse-Flow Combustor Performance with Liquid Fuel Injection" GT2006-91338 in Proceedings of the ASME/IGTI Turbo Expo 2006, May 8-11, 2006 Barcelona, Spain.

<sup>3</sup> M. K. Bobba, P. Gopalakrishnan, A. Radhakrishnan, J. Seitzman, Y. Neumeier, B. Zinn, and J. Jagoda "Flame Stabilization and Mixing Studies in a Novel Ultra-Low Emissions Combustor" AIAA-2006-963 44th AIAA Aerospace Sciences Meeting and Exhibit, Jan. 9-12, 2006 Reno, Nevada.

<sup>4</sup> Gopalakrishnan, P., Undapalli, S., Bobba, M., Sankaran, V., Menon, S., Zinn, B. T., Seitzman, J. M. "Measurements and Modeling of the flowfield in an Ultra-low emissions combustor," AIAA-2006-962 44th AIAA Aerospace Sciences Meeting and Exhibit, Jan. 9-12, 2006 Reno, Nevada.

<sup>5</sup> V. Sankaran, P. Gopalakrishnan, S. Undapalli, V. Parisi, J. M. Seitzman, and S. Menon "A LES – PIV Investigation of a Stagnation Point Reverse Flow Combustor," AIAA2005-3969 41st AIAA/ASME/SAE/ASEE Joint Propulsion Conference & Exhibit 10 - 13 July 2005, Tucson, Arizona.

<sup>6</sup> M. K. Bobba, P. Gopalakrishnan, J. M. Seitzman and B. T. Zinn "Characteristics of Combustion Processes in a Stagnation Point Reverse Flow Combustor" GT2006-91217 in Proceedings of the ASME/IGTI Turbo Expo 2006, May 8-11, 2006 Barcelona, Spain.

<sup>7</sup> P. Gopalakrishnan, M. K. Bobba and J.M. Seitzman "Controlling mechanisms for Low NO<sub>x</sub> Emissions in a Nonpremixed Stagnation Point Reverse Flow Combustor" Proc. of Comb. Inst.(2006).

<sup>8</sup> C. J. Lawn "Distributions of Instantaneous Heat Release by the Cross-Correlation of Chemiluminescent Emissions," *Combustion and Flame* 132 (2000) 227-240.

<sup>9</sup> R. J. Roby, A. J. Hamer, E. L. Johnsson, S. A. Tilstra and T. J. Burt "Improved Method for Flame Detection in Combustion Trbines" *Transactions of the ASME* 117 (1995) 332 –340.

<sup>10</sup> H. N. Najm, P. H. Paul, C. J. Mueller and P. S. Wyckoff *Combustion and Flame* 113 (3) (1998) 312-332.

<sup>11</sup> G. K. Mehta, M. K. Ramachandra and W. C. Strahle "Correlations between Light Emission, Acoustic Emission and Ion Density in Premixed Turbulent Flames" *Proc. Combust. Inst.* 18 (1980) 1051-1059.

<sup>12</sup> Kojima, J., Ikeda, Y., and Nakajima, T. "Spatially resolved measurement of OH\*, CH\* and C<sub>2</sub>\* chemiluminescence in the reaction zone of laminar methane/air premixed flames" Twenty eighth Symposium (International) on Combustion, 2000, pp. 1757-1764.

<sup>13</sup> Roby, R. J., Reaney, J. E., and Johnsson, E. L. "Detection of Temperature and Equivalence Ratio in Turbulent Premixed Flames Using Chemiluminescence" Proceedings of the 1998 Int. Joint Power Generation Conference, Vol. 1, 1998, 593-602.

<sup>14</sup> Ikeda, Y., Kojima, J., and Nakajima, T. "Chemiluminescence based local equivalence ratio measurement in turbulent premixed flames" AIAA-2002-0191, 40<sup>th</sup> Aerospace sciences meeting and exhibit, Reno, Nevada, Jan 14-17, 2002.

<sup>15</sup> M. R. Morrell, J. M. Seitzman, M. Wilensky, E. Lubarsky and B. Zinn "Interpretation of Optical Emissions for Sensors in Liquid Fueled Combustors" AIAA 2001-0787 39th AIAA Aerospace Sciences Meeting and Exhibit, Jan. 8-11, 2001 Reno, Nevada.

<sup>16</sup> T. M. Muruganandam, B.-H. Kim, M. R. Morrell, V. Nori, M. Patel, B. W. Romig and J. M. Seitzman, "Optical Equivalence Ratio Sensors for Gas Turbine Combustors" Proc. Combust. Inst. 30, pp. 1601-1609, The Combustion Institute (2005).